Effect of SPARC Suppression in Mice, Perfused Human Anterior Segments, and Trabecular Meshwork Cells

William W. MacDonald,[1] Swarup S. Swaminathan,[1,2] Jae Young Heo,[1] Alexandra Castillejos,[1,3] Jessica Hsueh,[1] Brian J. Liu,[1] Diane Jo,[1] Annie Du,[1] Hyunpil Lee,[1] Min Hyung Kang,[1] and Douglas J. Rhee[1]

[1]Department of Ophthalmology & Visual Sciences, University Hospitals, Case Western Reserve University School of Medicine, Cleveland, Ohio, United States
[2]Department of Ophthalmology, Bascom Palmer Eye Institute, Miami, Florida, United States
[3]Department of Ophthalmology, Massachusetts Eye & Ear Infirmary, Boston, Massachusetts, United States

Correspondence: Douglas J. Rhee, Department of Ophthalmology & Visual Sciences, 10900 Euclid Ave, Lakeside 4129, Cleveland, OH 44105, USA; douglas.rhee@uhhospitals.org.

Received: October 21, 2021
Accepted: April 25, 2022
Published: June 7, 2022

Citation: MacDonald WW, Swaminathan SS, Heo JY, et al. Effect of SPARC suppression in mice, perfused human anterior segments, and trabecular meshwork cells. *Invest Ophthalmol Vis Sci.* 2022;63(6):8. https://doi.org/10.1167/iovs.63.6.8

Purpose. Secreted protein, acidic and rich in cysteine (SPARC) elevates intraocular pressure (IOP), increases certain structural extracellular matrix (ECM) proteins in the juxtacanalicular trabecular meshwork (JCT), and decreases matrix metalloproteinase (MMP) protein levels in trabecular meshwork (TM) endothelial cells. We investigated SPARC as a potential target for lowering IOP. We hypothesized that suppressing SPARC will decrease IOP, decrease structural JCT ECM proteins, and alter the levels of MMPs and/or their inhibitors.

Methods. A lentivirus containing short hairpin RNA of human SPARC suppressed *SPARC* in mouse eyes and perfused cadaveric human anterior segments with subsequent IOP measurements. Immunohistochemistry determined structural correlates. Human TM cell cultures were treated with SPARC suppressing lentivirus. Quantitative reverse transcriptase polymerase chain reaction (PCR), immunoblotting, and zymography determined total RNA, relative protein levels, and MMP enzymatic activity, respectively.

Results. Suppressing SPARC decreased IOP in mouse eyes and perfused human anterior segments by approximately 20%. Histologically, this correlated to a decrease in collagen I, IV, and VI in both the mouse TM and human JCT regions; in the mouse, fibronectin was also decreased but not in the human. In TM cells, collagen I and IV, fibronectin, MMP-2, and tissue inhibitor of MMP-1 were decreased. Messenger RNA of the aforementioned genes was not changed. Plasminogen activator inhibitor 1 (PAI-1) was upregulated in vitro by quantitative PCR and immunoblotting. MMP-1 activity was reduced in vitro by zymography.

Conclusions. Suppressing SPARC decreased IOP in mice and perfused cadaveric human anterior segments corresponding to qualitative structural changes in the JCT ECM, which do not appear to be the result of transcription regulation.

Keywords: SPARC, shRNA suppression, extracellular matrix (ECM), intraocular pressure (IOP)

Glaucoma is a leading cause of blindness worldwide that affects more than 66 million individuals.[1] Primary open-angle glaucoma (POAG) is the second leading cause of irreversible blindness in the United States.[2,3] POAG is characterized by the degeneration of retinal ganglion cells that is strongly correlated to an elevated intraocular pressure (IOP).[4] IOP is maintained by the balance between aqueous humor production and drainage. Conventional outflow of aqueous humor drainage is primarily through the trabecular meshwork (TM) into Schlemm's canal.[5] The exact molecular and cellular processes responsible for the normal physiologic regulation of outflow resistance across the TM are not fully elucidated. However, the equilibrium between the synthesis and breakdown of extracellular matrix (ECM) within the juxtacanalicular region of the TM (JCT) strongly influences IOP.[6] Furthermore, alterations of the ECM within the JCT have been found to be a primary pathophysiologic association with POAG.[7] We believe that proteins known to regulate ECM equilibrium in other tissues will influence IOP.

Secreted protein, acidic and rich in cysteine (SPARC) is a nonstructural, secreted glycoprotein that is involved in the cellular regulation of ECM.[5] SPARC is significantly expressed in a variety of tissues and is implicated in a wide range of pathologic processes, including hepatic fibrosis,[8] osteoporosis,[9] and renal interstitial fibrosis,[10] in which fibrosis plays an important role. We and others have investigated the potential role of SPARC in IOP regulation and glaucoma.[11] SPARC is highly expressed in human TM in response to physiologic stress.[12] Furthermore, overexpression of SPARC elevates IOP in perfused human cadaveric

anterior chambers.[13] Conversely, *SPARC*$^{-/-}$ mice have a lower IOP and more uniform aqueous outflow.[11,14] One mechanism by which SPARC may increase resistance is by causing a qualitative change in the JCT ECM; SPARC overexpression increases collagen I, collagen IV, fibronectin,[15] and laminin in cultured TM cells and perfused human cadaveric anterior chambers.[13] Although the relative quantities of these proteins changed, their messenger RNA (mRNA) was not affected by SPARC overexpression,[13] indicating that regulation of these components by SPARC was unrelated to transcriptional control. SPARC overexpression decreased the level of pro–matrix metalloproteinase (MMP) 9 and MMP-9 enzyme activity, suggesting a possible mechanism.[13] These studies indicate that SPARC plays a critical regulatory role in normal TM outflow resistance.

Transforming growth factor β2 (TGF-β2) is highly increased in the aqueous humor of patients with POAG.[16,17] TGF-β2 itself increases IOP in experimental models.[18] In TM cells, SPARC is the most highly expressed protein in response to TGF-β2[19] through activation of Smad 2/3 and p38 pathways.[20] TGF-β2 is unable to increase IOP in *SPARC*$^{-/-}$ mice, strongly implicating SPARC as a critical component of the pathogenesis of POAG.[21]

We hypothesized that inhibiting SPARC will lower IOP and correspond to qualitative changes in certain structural ECM proteins and MMPs. We investigated the effect of suppressing *SPARC* using short hairpin RNA (shRNA) in mice, perfused cadaveric human anterior segments, and human TM endothelial cells.

Materials and Methods

Lentivirus Construction

A lentiviral shRNA kit was purchased from Open Biosystems, Inc. (Huntsville, AL, USA) in which five different shSPARC sequences (#8709, #8710, #8711, #8712, and #8713) were included. To screen out the most effective construct to downregulate SPARC expression in TM cells, 0.5 µg of the constructs was transfected into 297T and HT1080 cell lines. SPARC expression was analyzed by Western blot, in which the constructs (#8709, 5′-CGGTTGTTCTTTCCTCACATT-3′ for human SPARC; #8712, 5′-GTGAAGAAGATCCATGAGAAT-3′ for mouse SPARC) were chosen because they most effectively downregulated SPARC in the tumor cell lines. Then, lentivirus-expressing shRNA (#8709) (Lenti-shSPARC) was produced by transfecting the 293T cell line following the manufacturer's protocol. The day before transfection, the 293T cells were plated at a density of 5.5 × 10^6 cells per 100-mm plate. On the day of transfection, DNA/Arrest-In complexes were made by mixing 9 µg of construct DNA, 28.5 µg of packaging mix, and 187.5 µg of Arrest-In transfection reagent in 2 mL of serum-free media or plain Dulbecco's modified Eagle's medium (DMEM). After incubating the mixture for 20 minutes at room temperature (RT), 3 mL of Opti-MEM I Reduced Serum Medium (Thermo Fisher Scientific, Waltham, MA, USA) was added to the transfection complexes. It was mixed very gently and replaced onto the cells, which were incubated at 37°C, 5% CO_2 chamber for 3 to 6 hours. After the transfection mixtures were removed, 12 mL DMEM (10% fetal serum bovine, 1× penicillin/streptomycin and 1× L-glutamate) was replaced. Cells were then incubated at 37°C, 5% CO_2 chamber for 48 hours. Nonsilent (NS) shRNA was used to construct the nonsilent control lentivirus (Lenti-shControl) (5′-ATCTCGCTTGGGCGAGAGTAAG-3′). After 48 hours of incubation, lentivirus-including media were harvested. To purify and determine lentivirus titer, ViraBind Lentivirus Concentration and Purification kit and QuickTiter Lentivirus Quantitation kit (Cell Biolabs, Inc., San Diego, CA, USA) were used per the manufacturer's instructions. TM cells were infected using Lenti-shSPARC at 2 × 10^6 transduction units (TU)/mL (2 multiplicity of infection (MOI)) in DMEM media with 2% fetal bovine serum (FBS) including 8 µg/mL of polybrene (Sigma-Aldrich, St. Louis, MO). Then, the cells were incubated for 3 days and DMEM replaced with serum-free media for another 24 hours. The next day, cell lysates (CLs) and conditioned media (CM) were harvested to perform Western blot analysis or quantitative polymerase chain reaction (qPCR).

Murine Lentiviral Injection

All experiments using mice were in accordance with the ARVO Statement for the Use of Animals in Ophthalmic and Vision Research and an approved institutional animal care and use committee protocol at the Massachusetts Eye and Ear Infirmary and Case Western Reserve University. Wild-type (WT) strains (C57BL/6 × 129/SvJ) were obtained from the Benaroya Research Institute at Virginia Mason (Seattle, WA, USA). All mice were between the ages of 8 and 14 weeks, and injections were performed in a biosafety level 2 room. Mice were anesthetized with a ketamine/xylazine/acepromazine mixture (100 mg, 10 mg, 1 mg per kg of body weight, respectively; Patterson Veterinary Supply, Danvers, MA, USA). Control or shSPARC lentivirus was loaded in a Nanofil syringe (World Precision Instruments [WPI], Sarasota, FL, USA) and connected to a 36-gauge needle (NF36BV-2; WPI). The mouse was placed on a stereotactic stand (BrandTech Scientific, Essex, CT, USA). The needle was inserted intracamerally by penetrating the peripheral cornea as parallel to the iris as possible using a clear corneal beveled incision. The needle was positioned such that the lumen faced the center of the anterior chamber. Using a microprocessor-based micro-syringe pump controller (Micro4; WPI), 2 µL of lentivirus was injected intracamerally at a rate of 4 nL/s. Based on the injected volume and previous calculations of aqueous humor dynamics for mice of this age range,[22] a conservative estimate for complete aqueous turnover was calculated as 44 minutes. After the injection was completed, the needle remained in the eye for the additional 44 minutes to maintain the pressure gradient to allow the lentivirus to contact and infect TM. Lubricant drops (GenTeal, Alcon Laboratories Inc., Fort Worth, TX) were applied to the exterior of both eyes. After the 44-minute period elapsed, the needle was removed from the eye. Forceps were used to briefly grasp the cornea near the injection site to provide local tamponade. One drop of proparacaine (Alcaine; Alcon, Fort Worth, TX, USA) and one drop of ofloxacin (Akorn, Lake Forest, IL, USA) were then administered.

IOP Measurement

Rebound tonometry was used to measure IOP. Our measurement technique and its accuracy have been described in detail previously.[23] Briefly, the anesthetized mouse was placed on a movable stand (BrandTech Support Jack; BrandTech Scientific, Essex, CT, USA) with its nose inside a facemask. The TonoLab tonometer (Colonial Medical Supply,

Investigative Ophthalmology & Visual Science

Franconia, NH, USA) was fixed horizontally and a remote pedal was used to actuate measurements to eliminate potential artifact caused by manual handling of the device. A set of six measurements was repeated three times, and the mode of each set was averaged; this value was recorded as the IOP. All measurements and injection experiments were conducted between 11 AM and 3 PM to minimize potential artifact from circadian variability.[12,24] The IOP of both eyes was measured the day before injection and every other day after intracameral injection starting on the 4th and ending on the 13th day.

Tissue Processing and Histology

After determining the overall IOP trend in a cohort of WT mice injected with Lenti-shSPARC over approximately 2 weeks, the lowest IOP was noted to be 8 days after injection. Another cohort of mice was subsequently injected with control or Lenti-shSPARC for morphologic analysis specifically at this time point of 8 days. At 8 days, this cohort was euthanatized with CO_2, and their eyes were enucleated immediately for fixation in 10% paraformalin (VWR International, Radnor, PA, USA) for 24 hours at RT, followed by transfer to 70% ethanol at 4°C. Eyes were then processed and embedded in paraffin wax for serial sectioning of 5-µm-thick sections, which were stained with hematoxylin and eosin and for immunohistochemistry studies.

Human Perfused Anterior Segment Culture System

Our technique has previously been described in detail.[20] Briefly, pairs of ocular disorder-free human donor eyes (ages 59, 62, and 71 years) were obtained from regional eye banks and managed according to the Declaration of Helsinki guidelines on research involving human tissue and our institutional review board. Anterior segments were isolated from the rest of the eyes. The irises and lenses were removed as well. The anterior segments were rinsed with culture medium consisting of DMEM with 1% FBS, 1% L-glutamine (2 mM), penicillin (100 U/mL), streptomycin (100 U/mL), gentamicin (0.17 mg/mL), and amphotericin-B (0.25 µg/mL). The anterior segments were mounted in custom plexiglass culture chambers, and microinfusion pumps (Harvard Apparatus, Holliston, MA, USA) were used to perfuse the segments at a constant flow rate of 2.5 µL/min with the previously described culture medium under 5% CO_2 at 37°C. IOP was monitored with a pressure transducer (BD Medical, Franklin Lakes, NJ, USA), and hourly averages of measurements taken every second were recorded. After a stable baseline IOP was achieved, one eye of each pair was injected with Lenti-shControl and the other eye with Lenti-shSPARC using 1×10^8 infectious units in 100 µL. Perfusion and IOP measurements were continued for 5 days, after which the anterior segments were fixed and sectioned for subsequent light microscopy and immunohistochemistry studies.

Immunohistochemistry

The following antibodies were used in this study: collagen I (600-401-103-0.1; Rockland, Gilbertsville, PA, USA), collagen IV (AB756P; EMD Millipore, Billerica, MA, USA), collagen VI (SAB4500387; Sigma-Aldrich), fibronectin (ab23750; Abcam, Cambridge, MA, USA), laminin (AB2034; EMD Millipore), and SPARC (AF942; R&D Systems, Minneapolis, MN, USA). Sections were washed with xylene and subsequently hydrated with ethanol dilutions (100%, 95%, 70%) three times. Sections were then rinsed with deionized H_2O. Tissue was then blocked in 10% donkey serum (all other antibodies) for 1 hour at RT and permeabilized using 0.2% Triton-100. Primary antibody was applied at 1:100 concentration overnight at 4°C. Slides were subsequently washed with 1× Phosphate Buffered Saline with Tween20 (PBS-T), and 1:200 secondary antibody was applied for 1 hour at RT (Table 1). Slides were washed once again, and the tissue was imaged using the Zeiss Axiovert 200M inverted fluorescent microscope (Carl Zeiss, Heidelberg, Germany) attached to a digital camera (AxioCam MR3; Carl Zeiss). Images were obtained using the associated software (Axiovision 4.8.2; Carl Zeiss). Slides of tissue from control and experimental interventions were imaged at the same time using the same control slide to normalize the intensity of staining.

Fluorescence Intensity Measurements for Human JCT Region and Mouse TM Region

Quantification of fluorescence was performed using a previously established methodology.[13,25–27] Briefly, for human tissue, the section stained with secondary antibody only was used to identify optimal exposure times for target ECM proteins (Alexa Fluor 488, Thermo Fisher Scientific Inc., Waltham, MA) that would eliminate signal due to nonspecific binding. These exposure times were used to image fluorescence from the target protein in all other sections. Three areas within the human JCT region were selected at random for each section, and ImageJ (National Institutes of Health, Bethesda, MD, USA) was used to calculate the average fluorescence in the 488 and 594 channels using a rectangle with consistent dimensions (0.40w × 1.20h).[26] Similarly, for the mouse TM region, the section only stained with secondary antibody was used to identify optimal exposure time for target ECM proteins (Alexa Fluor). Instead of rectangles, circles with consistent dimensions (0.28w × 0.28h) were used. This corresponded to an image area of 78.5 μm^2. Fifteen areas within a single mouse TM region were randomly selected but avoided areas of obvious artifactual punctate bright staining. Average fluorescence was measured for $N = 1$. Sections from different mice were sampled for additional N values.

Human TM Cell Culture/RNA and Protein Extraction and Isolation

Human TM cells were isolated from dissected human TM tissue explants derived from normal donors. All donor tissues were obtained from regional eye banks and managed according to the Declaration of Helsinki guidelines on research involving human tissue and our institutional review board. TM cells were isolated, propagated, and maintained according to recent TM cell culture consensus guidelines.[28] For maintenance, cells were in DMEM supplemented with 20% FBS, 1% L-glutamine (2 mM), and 0.1% gentamicin (50 µg/mL). TM cultures were seeded in standard-sized Petri dishes and grown to confluence at 37°C in 10% CO_2. Purified RNA and protein were extracted from CM and CL from TM cell cultures following protocol for the IBI DNA/RNA/protein extraction kit (IBI Scientific, Peosta, IA, USA).

Investigative Ophthalmology & Visual Science

Table 1. Primary and Secondary Antibodies Used for Immunoblot and Immunofluorescence in This Study

Primary Antibody	Company	Antibody Host	Dilution
Immunoblot			
MMPs			
MMP-1	R&D Systems	Mouse	1:1000
MMP-2	R&D Systems	Mouse	1:1000
MMP-3	R&D Systems	Goat	1:1000
MMP-9	R&D Systems	Mouse	1:1000
ECM			
Collagen I	Novus	Rabbit	1:1000
Collagen IV	Abcam	Rabbit	1:1000
Collagen VI	Sigma-Aldrich	Rabbit	1:1000
Fibronectin	Sigma-Aldrich	Mouse	1:1000
Laminin	Sigma-Aldrich	Mouse	1:1000
TIMPs			
TIMP-1	Chemicon	Rabbit	1:1000
TIMP-2	Cell Signaling	Rabbit	1:1000
TIMP-3	R&D Systems	Mouse	1:1000
TIMP-4	R&D Systems	Goat	1:1000
Others			
PAI-1	Cell Signaling	Rabbit	1:1000
SPARC	Haematologic Technologies	Mouse	1:10,000
Immunofluorescence			
ECM			
Collagen I	Rockland	Rabbit	1:100
Collagen IV	EMD Millipore	Rabbit	1:100
Collagen VI	Sigma-Aldrich	Rabbit	1:100
Fibronectin	Abcam	Rabbit	1:100
Laminin	EMD Millipore	Rabbit	1:100
Others			
SPARC	R&D Systems	Goat	1:500
Secondary Antibody	Company	Dilution	
Immunoblot			
IRDye 680 anti-mouse	Rockland	1:10,000	
IRDye 680 anti-rabbit	Rockland	1:10,000	
IRDye 680 anti-goat	Rockland	1:10,000	
IRDye 800 anti-mouse	Rockland	1:10,000	
IRDye 800 anti-rabbit	Rockland	1:10,000	
Immunofluorescence			
Goat anti-goat 488	Thermo Fisher	1:200	
Goat anti-rabbit 488	Thermo Fisher	1:200	
Goat anti-goat 594	Thermo Fisher	1:200	
Goat anti-rabbit 594	Thermo Fisher	1:200	

Immunoblotting

CM from primary TM cell cultures were harvested. The CLs from primary TM cell cultures were lysed in 1× radioimmunoprecipitation assay buffer (150 mM NaCl, 1% Igepal, 0.5% sodium deoxycholate, 0.1% sodium dodecyl sulfate [SDS], 50 mM Tris-HCl, pH 8.0) and collected. Equal amounts of total protein from CM and CL were mixed with 6× reducing buffer to a total of 36 µL. The solution was boiled for 5 minutes to denature the proteins. Then, 30 µL of each sample was loaded in 10% polyacrylamide gels for electrophoresis. SDS-PAGE was run at 150 V in tank buffer (25 mM Tris-HCl, 250 mM glycine, 0.1% SDS). The separated proteins were then transferred to a nitrocellulose membrane with a 0.46-µm pore size in blotting buffer (250 mM Tris-HCl, 192 mM glycine, and 10% methanol). The membrane was incubated for 1 hour in 0.5× blocking buffer at RT and treated with primary antibody overnight at 4°C. Antibodies to MMP-1, MMP-2, MMP-3, and MMP-9 detected the active forms of the matrix metalloproteinases. The next day, the membrane was washed three times for 10 minutes each wash in TBS-T (50 mM Tris-HCl, 150 mM NaCl, 0.05% Tween-20). The secondary antibody, IRDye 800–conjugated IgG, was added for 1 hour at RT. The membrane was once again washed three times for 10 minutes each wash. The membrane was scanned for analysis of band density via the Odyssey Li-Cor System (Odyssey DLx Imaging System LI-COR Inc., Lincoln, NE).

Zymography

CM from primary TM cell cultures were harvested. Equal amounts of total protein from CM were mixed with 6× nonreducing buffer to a total of 36 µL. Then, 30µL of each sample was loaded in 10% polyacrylamide gels for electrophoresis. During casting of gels, gelatin (2%) for MMP-2 or β-casein (2%) for MMP-1 was mixed into liquid acrylamide. Samples were run at 150 V in tank buffer (25 mM Tris-HCl, 250 mM glycine, 0.1% SDS). The gels were incubated with 2.5% Triton X-100 (renaturing buffer) at RT, then transferred to enzyme assay buffer (50 mM Tris-HCl [pH 7.5], 150 mM NaCl, 5 mM $CaCl_2$, 0.02% Brij35, 0.05% NaN_3) overnight at 37°C. The next day, gels were stained with 0.1% Coomassie

Investigative Ophthalmology & Visual Science

Brilliant Blue G-250 (Bio-Rad, Hercules, CA, USA) for at least 3 hours and were then destained with fixing/destaining solution until clear bands were visible and contrasted well with the blue background. The gel was scanned for analysis of band density via the Odyssey Li-Cor System. The MMPs were identified based on their molecular weights and confirmed against purified MMP-1 and MMP-2 (Chemicon, Temecula, CA, USA) as positive controls.

cDNA Synthesis

In total, 500 ng RNA was added to 500 ng oligo(dT) and RNase-free water sufficient to equal a total volume of 10 µL. The mixture was heated at 65°C for 5 minutes to denature the RNA. Then, 1 µL of dNTP, 1 µL of reverse transcriptase, 1 µL of primer, 10 µL of M-MLV reaction mix, and 27 µL of RNase-free water were added into the mixture. The reaction mixture was incubated at 42°C for 1 hour to synthesize cDNA and then used for qPCR. Otherwise, the mixtures were stored at −20°C.

Quantitative RT-PCR

A mixture of 7 µL RNase-free water, 10 µL SYBR green reaction mix, 2 µL target forward and reverse primers, and 1 µL sample cDNA were added to each well of the PCR plate. Each combination of target primers and sample cDNA was run in triplicate. The plate was run using a StepOnePlus Real-Time PCR (Thermo Fisher Scientific Inc., Waltham, MA) machine. Experimental gene levels were normalized to the housekeeping gene (β-actin) using the $2^{-\Delta\Delta Ct}$ method.

Statistical Analysis

Paired two-tailed Student's *t*-tests were performed using Microsoft Excel (Microsoft, Redmond, WA, USA) and GraphPad Prism version 6.00 for Windows (GraphPad Software, La Jolla, CA, USA). $P < 0.05$ was considered statistically significant. Average percentage change from control, standard deviation, and significance calculations were conducted.

Results

Effect of shRNA-Induced SPARC Suppression on Mouse IOP

Suppression of SPARC with Lenti-shSPARC significantly decreased the IOP in mouse eyes compared to those injected with Lenti-shControl from days 6 to 20 postinjection (Fig. 1A). There was approximately a 20% decrease in IOP for mice injected with Lenti-shSPARC compared to the IOP of uninjected eyes (Fig. 1B) from days 6 to 24

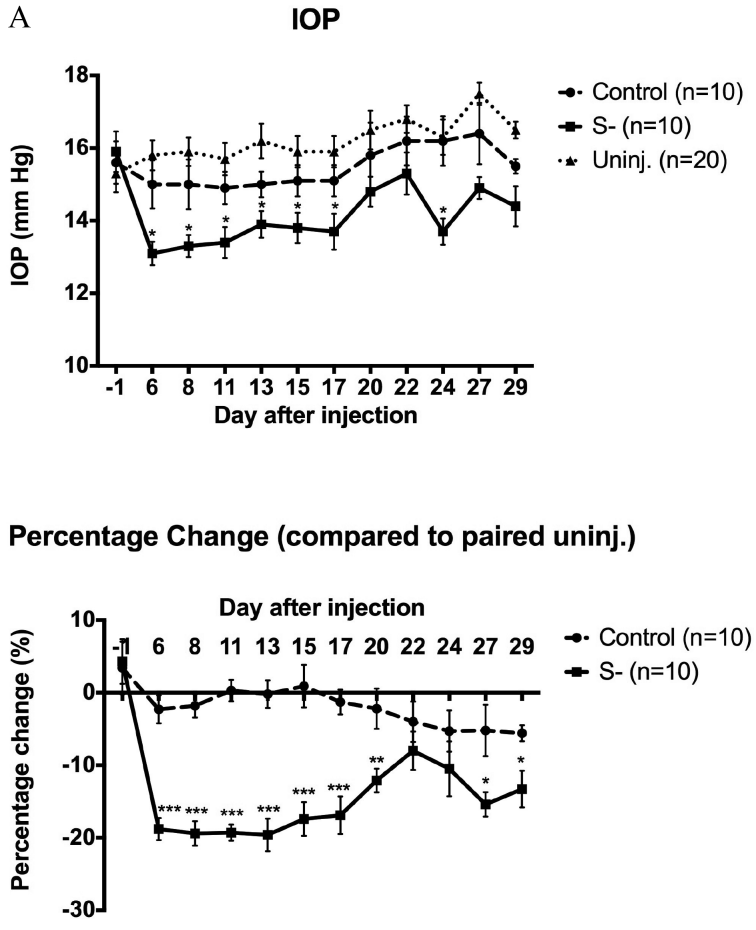

Figure 1. Effect of SPARC suppression on mouse IOP: IOP measurement (**A**) and percent change (**B**) (compared to paired uninjected eyes) in mice after Lenti-shSPARC or Lenti-shControl treatment. There was a significant decrease of IOP in eyes treated with Lenti-shSPARC compared to the IOP of eyes treated with Lenti-shControl from days 6 to 20 postinjection.

Investigative Ophthalmology & Visual Science

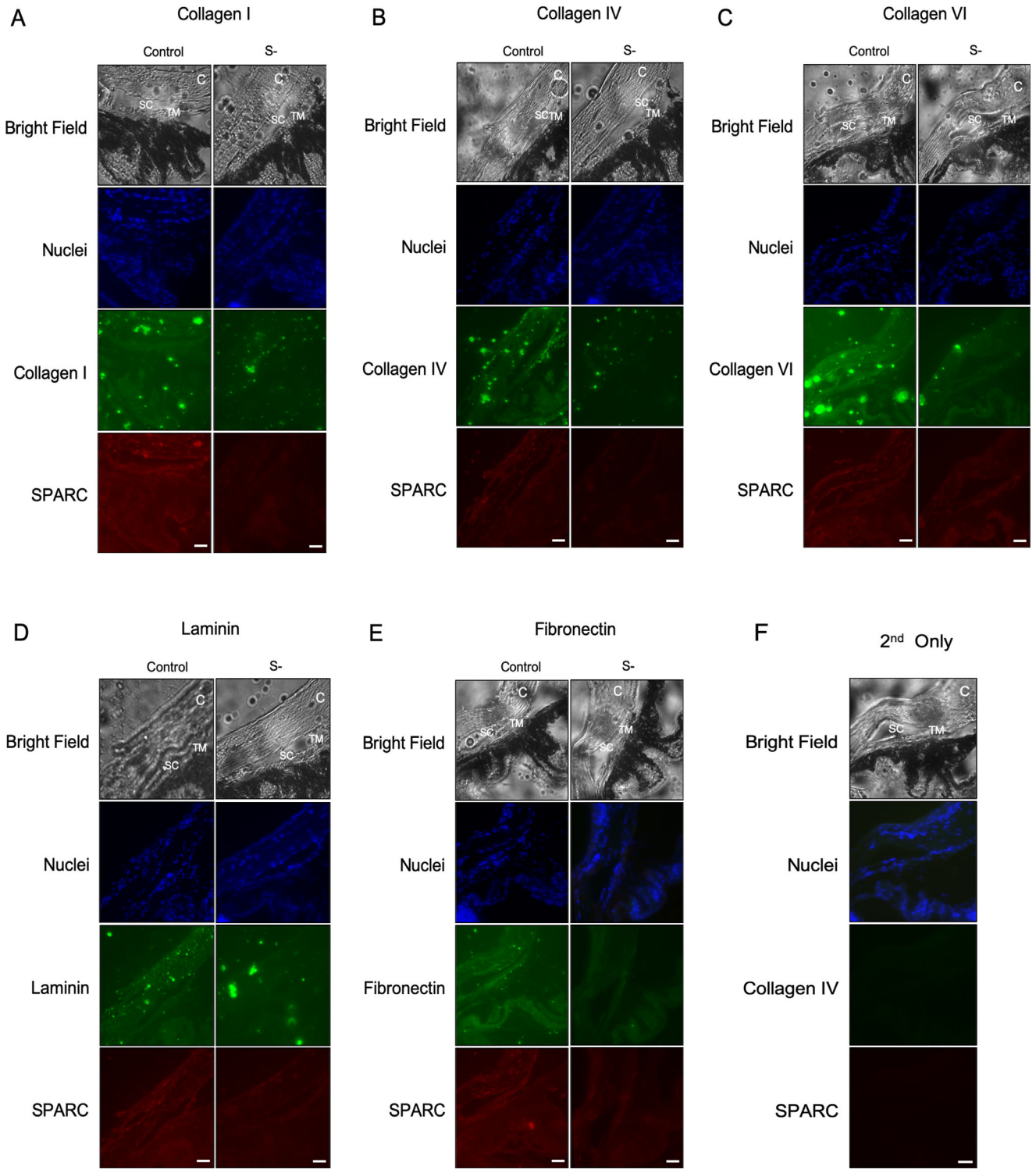

Figure 2. Representative immunolabeling of ECM proteins after infection with Lenti-shControl and Lenti-shSPARC (in vivo): collagen I (**A**), collagen IV (**B**), and collagen VI (**C**) and fibronectin (**E**) decreased in response to Lenti-shSPARC, but laminin (**D**) was unchanged. SPARC was detected in S- due to the partial suppression of SPARC by Lenti-shSPARC. The secondary only staining (**F**) is shown as a negative control. *Scale bar*: 40 µm. Control, Lenti-shControl; S-, Lenti-shSPARC; SC, Schlemm's canal; TM, trabecular meshwork. Magnification 40×.

postinjection. There was no significant difference between the IOPs of eyes that received the Lenti-shControl and the uninjected control eyes ($P > 0.05$).

Immunohistochemistry (IHC) of the mouse eye sections revealed that SPARC was decreased −38.6% ± 15.6% by Lenti-shSPARC infection (Fig. 2 and Table 2) compared to uninjected eyes. In these mouse sections, fibronectin and collagen I, IV, and VI were decreased compared to Lenti-shControl (Fig. 2 and Table 2). Laminin was not affected (Fig. 2 and Table 2).

Investigative Ophthalmology & Visual Science

Table 2. Fluorescence Intensity Measurements of ECM and SPARC Proteins in the TM Region Following Injection of Lenti-shSPARC in Mice

	Lenti-shSPARC		
	% Change, Mean ± SD	*n*	*P* Value
SPARC	−38.6 ± 15.6	5	0.0007*
Collagen I	−22.3 ± 14.3	3	0.004*
Collagen IV	−21.1 ± 12.3	3	0.003*
Collagen VI	−19.0 ± 7.4	3	0.002*
Fibronectin	−15.3 ± 8.2	3	0.03*
Laminin	−2.3 ± 8.7	3	0.71

The percent (%) change in Lenti-shSPARC treatment was normalized with Lenti-shControl. The arbitrary fluorescence unit from the ImageJ software was used. SPARC, fibronectin, and collagen I, IV, and VI in the TM region of mouse eyes were decreased with Lenti-shSPARC injection.

* Statistically significant.

Effect of SPARC Suppression in Perfused Human Anterior Segments

Ex vivo experiments were carried out with three pairs of donor eyes 59, 62, and 71 years of age without any ocular or infectious diseases. Suppressing SPARC with Lenti-shSPARC significantly decreased the IOP in human anterior segments compared to the IOP in those treated with Lenti-shControl beginning 96 hours postinfection ($P = 0.008$) through the end of the measured time (i.e., 125 hours; Fig. 3). Histologic review of random sections following similarly published protocols did not reveal any obvious changes in TM cellularity to warrant more formal studies to assess any change in TM cellularity as a possible confounding cause for the IOP-lowering effect (Fig. 4).[29,30] There were no grossly obvious anatomic changes visible on microscopy of the anterior chamber angles.

Effect of SPARC Suppression on ECM Proteins in Perfused Human Anterior Segments

After completion of perfusion, IHC of the anterior segments revealed that SPARC was decreased −33.6% ± 9.7% by Lenti-shSPARC infection (Fig. 5 and Table 3) in the JCT region. In these segments, collagen I, IV, and VI were decreased compared to Lenti-shControl (Fig. 5 and Table 3). Fibronectin and laminin were unaffected (Fig. 5 and Table 3).

Effect of SPARC Suppression on ECM, MMP, and TIMP Protein Levels and MMP Activity in Human TM Cells

In the conditioned media, SPARC protein was suppressed by Lenti-shSPARC at MOI 50 ($P < 0.0001$) compared to Lenti-shControl (NS) treated TM cells (Fig. 6). Suppression of SPARC decreased collagen I, collagen IV, and fibronectin but did not change laminin protein levels compared to Lenti-shControl (Table 4). Lenti-shSPARC also decreased MMP-2 levels and TIMP-1 levels and increased MMP-3 levels compared to Lenti-shControl; MMP-1 and MMP-9 as well as TIMP-2 through TIMP-4 were unchanged (Fig. 6 and Table 4). The net effect of the MMP and TIMP protein changes was a decrease of MMP-1 activity (Table 5 and Fig. 7).

Effect of SPARC Suppression on the Relative Levels of ECM, MMP, TIMPs, and PAI-1 Transcripts in Human TM Cells

Following Lenti-shSPARC or Lenti-shControl infection, the human TM cells showed no significant changes in any ECM mRNAs (Table 6). Additionally, there were no significant changes in any MMPs or TIMP mRNAs. However,

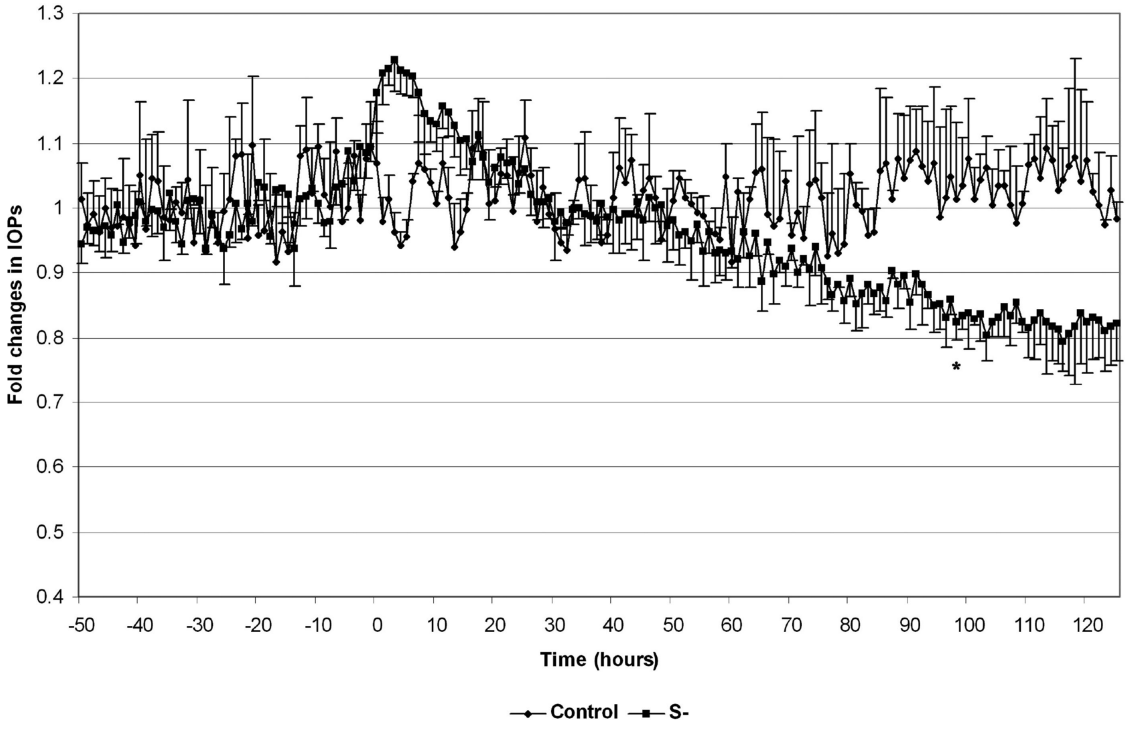

Figure 3. IOP of the perfused human anterior chamber segments: the segments treated with Lenti-shSPARC had a lower IOP beginning at hour 96 following treatment compared to segments that received Lenti-shControl ($n = 3$, $P = 0.008$ at hour 96; $P < 0.01$ for all time points from hours 96 through 125).

Investigative Ophthalmology & Visual Science

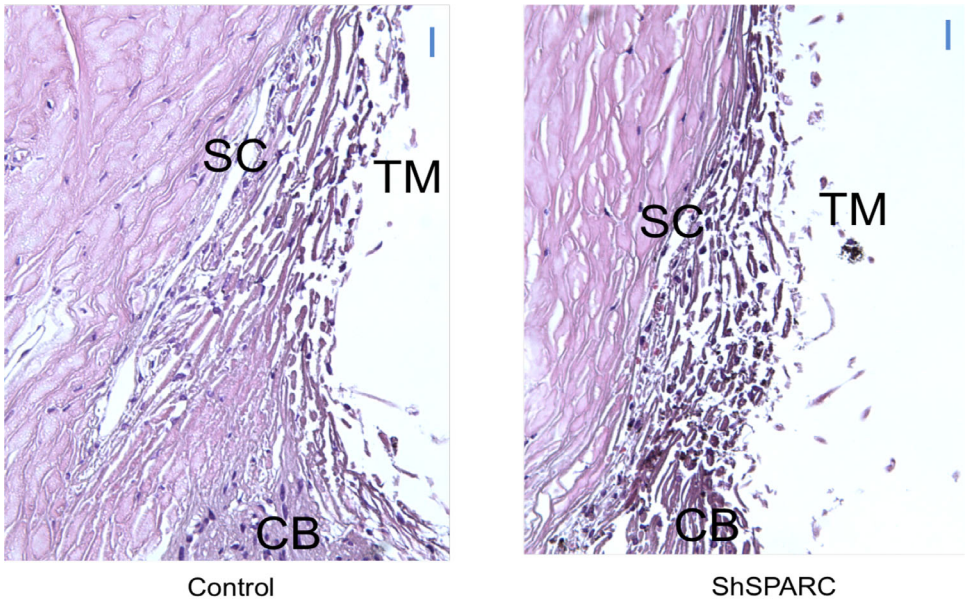

Figure 4. Representative hematoxylin and eosin stained sections of the perfused human anterior chamber segments treated with either Lenti-shControl or Lenti-shSPARC: there was no apparent qualitative difference in the cellularity of TM tissues infected. *Scale bar*: 20 µm. CB, ciliary body; Control, Lenti-shControl; SC, Schlemm's canal; ShSPARC, Lenti-shSPARC; TM, trabecular meshwork. Magnification 40×.

Lenti-shSPARC upregulated PAI-1 mRNA by 2.89 ± 1.14-fold ($P = 0.0096$) compared to that of Lenti-shControl treatment (Table 6).

Discussion

The goal of these studies was to investigate the physiologic impact of SPARC suppression in multiple model systems and ascertain structural correlations. We found that inhibiting *SPARC* in adult mice (in vivo) and adult human tissue (ex vivo) lowered IOP, providing preclinical proof of concept that inhibiting SPARC may be a reasonable therapeutic target to lower IOP.

We understand that there are limitations to using IHC stains to quantify our data. IHC stains are not standardized worldwide, and selectively choosing areas of interest can lead to selection bias. However, structurally, there was a consistent decrease of collagen I and IV in the immunohistochemical analysis of mouse eyes, ex vivo perfused human cadaveric anterior segments, and cultured TM cells. Moreover, collagen I and IV were increased in ex vivo perfused human cadaveric anterior segments and cultured TM cells when SPARC was overexpressed (SPARC overexpression in mice has not been reported).[13] Collectively, these data strongly implicate collagen I and IV as the key structural ECM proteins mediating the effects of SPARC. In the JCT TM, collagen IV is one of the principal components of the basement membrane in addition to fibronectin and laminin.[31] Glucocorticoid-induced POAG causes an increase in collagen IV along with an associated increase in IOP.[32] Mutated collagen I in mouse TM has also been shown to decrease ECM turnover and increase IOP.[33] Two single-nucleotide polymorphisms of collagen VI have been identified by a genome-wise association study of elevated IOP—rs7599762 COL6A3, which was decreased, and rs2839082 COL6A1-COL6A2, which was increased.[34] Whole-genome sequencing identified COL6A3 in a large family with POAG.[35] Primary cultures of TM cells isolated from eyes with glaucoma demonstrate an altered collagen VI distribution.[35] The decrease in collagen I and IV seen in our experiments correlates with increased TM outflow and is likely an important contributor to decreased IOP by SPARC suppression.

In the current study, collagen VI was decreased in the in vivo and ex vivo model systems (i.e., mice and perfused human anterior segments) but not in vitro. The difference seen in vitro may be related to the different environments between isolated cell culture instead of in situ with the surrounding tissue, ECM, and so on. With SPARC overexpression, collagen VI was increased, but only in cultured TM cells, and was unaffected in the IHC of perfused human anterior segments. Collagen VI is a significant component of the basement membrane of the JCT and is in greater quantities in glaucomatous eyes compared to normal eyes.[36] The decrease in collagen VI by SPARC suppression suggests a role in decreasing IOP.

Fibronectin decreased in TM cells and mouse eyes in response to SPARC suppression but did not change in perfused human anterior segments; when SPARC is overexpressed, fibronectin increases in both cultured TM cells and perfused human anterior segments.[13] Given fibronectin's important role in ECM assembly and IOP in TM, fibronectin likely plays a vital role in SPARC's effect on IOP.[37]

Laminin was not changed by SPARC suppression in any of our in vitro, ex vivo, or in vivo models; SPARC overexpression increased laminin only in cultured TM cells, indicating that laminin, although an important feature of the incomplete basement membrane within the JCT region, is not likely altered by SPARC.[31]

The mechanistic pathways by which SPARC mediates expression of ECM proteins in the TM is not fully elucidated. The mRNA levels of these ECM proteins were not changed in response to SPARC suppression, indicating that the mechanism is not a simple decrease in production. SPARC may act as a chaperone (i.e., a posttranslational

Investigative Ophthalmology & Visual Science

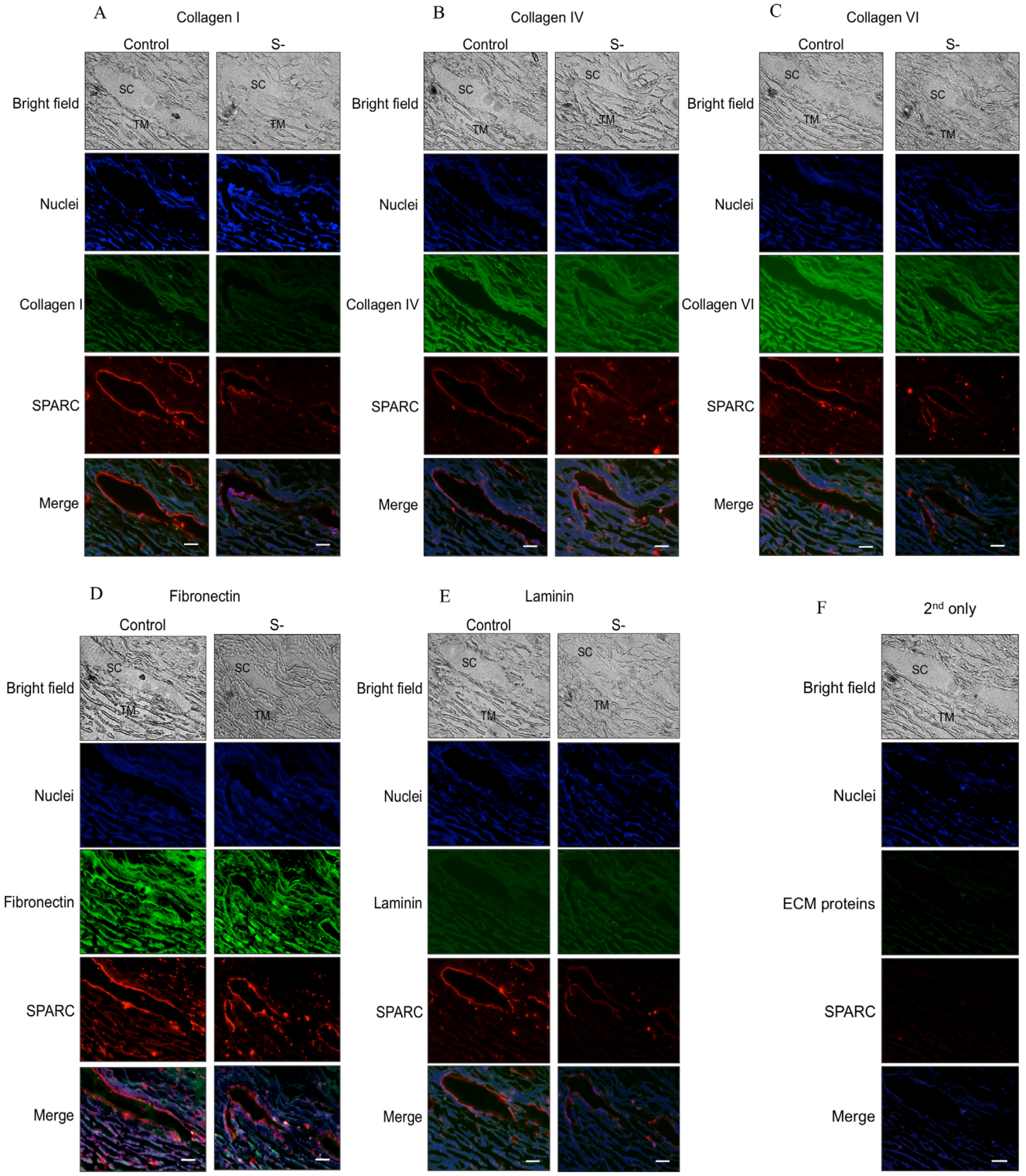

Figure 5. Representative immunolabeling of ECM proteins after infection with Lenti-shControl or Lenti-shSPARC of perfused human anterior chamber segments (ex vivo): collagen I (**A**), collagen IV (**B**), and collagen VI (**C**) were decreased, but fibronectin (**D**) and laminin (**E**) were not changed. SPARC was detected in S- due to the partial suppression of SPARC by Lenti-shSPARC. The secondary only staining (**F**) is shown as a negative control. *Scale bar*: 20 µm. Control, Lenti-shControl; S-, Lenti-shSPARC; SC, Schlemm's canal; TM, trabecular meshwork. Magnification 40×.

control to stabilize ECM proteins or mRNA, allowing for selective accumulation).[38] In TM pathways, maintenance of MMP and TIMP balance influences aqueous drainage and IOP. Perfusing MMP-2, MMP-3, or MMP-9 through human anterior segments increases outflow facility.[39] In cultured TM cells, SPARC suppression resulted in decreased MMP-

Table 3. Fluorescence Intensity of ECM and SPARC Proteins in the JCT Region From IHC of Perfused Human Anterior Chamber Segments After Injection of Lenti-shSPARC

	Lenti-shSPARC		
	% change, Mean ± SD	*n*	*P* Value
SPARC	−33.6 ± 9.7	5	0.00005*
Collagen I	−32.2 ± 10.6	5	0.0001*
Collagen IV	−25.51 ± 15.3	5	0.006*
Collagen VI	−29.0 ± 7.4	5	0.00002*
Fibronectin	−5.3 ± 21.2	5	0.59
Laminin	−1.0 ± 15.1	5	0.91

The percent (%) change in Lenti-shSPARC treatment was normalized with Lenti-shControl. Arbitrary fluorescence units from the ImageJ software were used for the data. SPARC and collagen I, IV, and VI were decreased.

* Statistically significant.

Table 4. Percent Change (%) of the Protein Levels of Selected MMPs and TIMPs Following SPARC Suppression in TM Cell Culture Conditioned Media Relative to Lenti-shControl

	shSPARC, Mean ± SD	*n*	*P* Value
ECM			
Collagen I	−44.20 ± 19.00	3	0.016*
Collagen IV	−74.00 ± 7.00	3	0.0004*
Fibronectin	−20.00 ± 1.90	3	0.003*
Laminin	−2.00 ± 11.00	3	0.75
MMPs			
MMP-1	26.75 ± 101.23	5	0.59
MMP-2	−59.94 ± 26.46	7	0.0004*
MMP-3	84.55 ± 122.31	8	0.046*
MMP-9	6.08 ± 39.57	7	0.37
TIMPs			
TIMP-1	−34.19 ± 40.94	7	0.035*
TIMP-2	−0.63 ± 23.45	5	0.48
TIMP-3	−8.46 ± 16.65	5	0.32
TIMP-4	12.36 ± 24.89	5	0.24
Others			
PAI-1	79.80 ± 66.38	6	0.032*

Fibronectin, collagen I and IV, and MMP-2 and TIMP-1 were decreased while MMP-3 and PAI-1 were increased.

* Statistically significant.

2 and TIMP-1 as well as an increase in MMP-3. Neither MMP nor TIMP transcript levels were affected by SPARC suppression. The selective change in MMP and TIMP levels with SPARC suppression suggests a qualitative change in JCT ECM composition rather than an overt decrease in ECM content. We did not see a significant change in expression of MMP-1 or MMP-9. By zymography, the net effect of decreased levels of both MMP-2 and TIMP-1 was the absence of change in MMP-2 activity; TIMP-1 is both an activator and inhibitor of pro-MMP-2.[40] Paradoxically, zymography demonstrated a decrease of MMP-1 activity. This could be partially explained by the PAI-1 fibrinolytic pathway, as will be discussed in the subsequent paragraph,[41] but further investigation is needed. SPARC overexpression

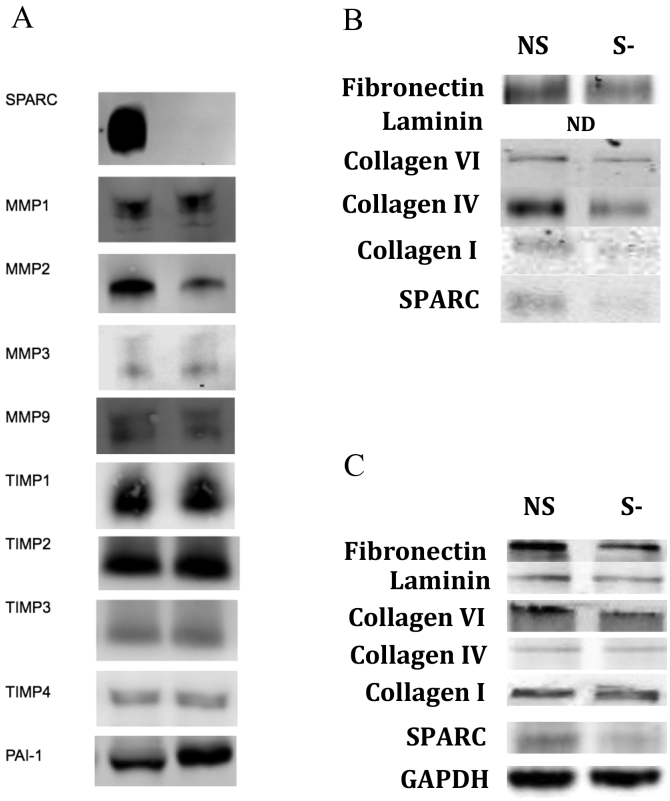

Figure 6. Representative immunoblots demonstrating the relative changes of SPARC, MMPs, and TIMPs induced by SPARC suppression using the lentivirus-expressing shRNA (S-) in TM cells. (**A**) In the conditioned media, MMP-2 was decreased by −59.94% ± 26.46%, TIMP-1 was decreased by −34.19% ± 40.94%, and MMP-3 was increased by 84.55 ± 122.31%. Expression of PAI-1 was also increased by 79.79 ± 66.38%. Immunoblots demonstrating relative changes in the levels of selected ECM proteins induced by SPARC suppression in the cell media of TM cells (**B**) as well as the cell lysate (**C**). ND, not detected.

Investigative Ophthalmology & Visual Science

Table 5. Percent Change (%) in the Activity of Selected MMPs Following SPARC Suppression in TM Cells

MMP	% Change vs. WT, Mean ± SD	*n*	*P* Value
MMP-1	−20.02 ± 16.95	6	0.03*
MMP-2	13.49 ± 28.90	6	0.3

As measured by zymography, MMP-1 activity was decreased.

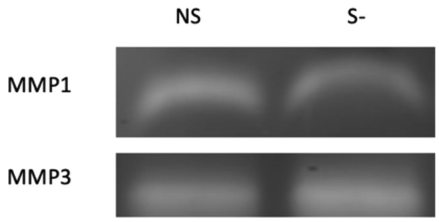

Figure 7. Representative zymography demonstrating the relative changes of MMPs induced by SPARC suppression using the lentivirus expressing shRNA (S-) in TM cells.

Table 6. Fold Changes of mRNA Levels of Selected ECM Proteins, MMPs, and TIMPs Compared to Control Following Infection by Lenti-shControl or Lenti-shSPARC

	shSPARC, Mean ± SD	*n*	*P* Value
Matricellular			
SPARC	−1.68 ± 0.37	8	0.0005*
ECM			
Collagen I	−0.43 ± 0.23	8	0.09
Collagen IV	0.22 ± 0.33	8	0.52
Collagen VI	−0.13 ± 0.16	8	0.45
Fibronectin	−0.13 ± 0.14	8	0.38
Laminin	0.10 ± 0.07	8	0.21
MMPs			
MMP-1	0.00 ± 0.48	5	0.99
MMP-2	−0.20 ± 0.33	5	0.25
MMP-3	0.06 ± 0.59	5	0.84
MMP-9	−0.04 ± 0.37	5	0.84
TIMPs			
TIMP-1	−0.04 ± 0.37	5	0.84
TIMP-2	0.03 ± 0.34	5	0.85
TIMP-3	−0.37 ± 0.72	5	0.30
TIMP-4	0.13 ± 0.40	5	0.49
Others			
PAI-1	0.95 ± 0.39	5	0.003*

SPARC mRNA was reduced (positive control) and PAI-1 mRNA was increased.

decreased MMP-9 and concurrently increased TIMP-1[13]; at a higher viral titer to further increase SPARC expression, MMP-1, MMP-3, and MMP-9 were decreased while TIMP-1 and TIMP-3 increased. It is possible that the SPARC suppression caused the observed decrease of fibronectin and collagen IV through increased MMP-3 activity; fibronectin and collagen IV are primary substrates for MMP-3 (stromelysin 1).[42] Previously, we showed that TM cells also express MMP-11, MMP-12, MMP-14, MMP-15, MMP-16, MMP-17, MMP-19, and MMP-24[43]; it is also possible that some of the other MMPs could also be affected by SPARC. Lack of SPARC in mice liver cells is associated with an increase in hepatic MMP-2 expression, indicating a similar effect on MMP-2 in other tissues.[44]

Experiments specifically designed to explore the molecular mechanisms by which SPARC exerts its effect are forthcoming and beyond the scope of the article. However, it does not appear that SPARC alters the aforementioned structural ECM proteins through alterations of transcription as we did not find any differences in relative levels of mRNA resulting from SPARC suppression.

Suppressing SPARC increased PAI-1 at the mRNA and protein levels; paradoxically, SPARC overexpression also increased PAI-1.[13] PAI-1 is an inhibitor of tissue plasminogen activator (tPA), a serine protease observed in the TM, corneal endothelium, and vascular endothelium of human eyes[45] that catalyzes the conversion of plasminogen to plasmin. Plasmin catalyzes the conversion of MMP-1, MMP-2, and MMP-9 to their active form.[46] tPA deficiency in mice is associated with reduced outflow facility and a decrease in MMP-9.[47] Additionally, SPARC's inducing effect on PAI-1 has been implicated in other tissues, including the lungs[48] and prostate.[41] It has also been shown that TGF-β2 causes an increase in PAI-1 production in human and bovine TM cells,[49,50] as well as human prostate cells.[51] TGF-β2 is upregulated in glaucomatous eyes[16,18] and also increases SPARC production.[20] In this study, shSPARC was associated with a significant increase in PAI-1 mRNA and protein levels in vitro, suggesting increased tPA inhibition and corresponding to the significant decrease in MMP-2 protein level. The seemingly paradoxical activity of PAI-1 has been observed before; in fibrosis, increasing PAI-1 inhibits urokinase-type/tissue-type plasminogen activator, plasmin, and plasmin-dependent MMPs, which generally causes increasing fibrosis and is implicated in pathology of the heart, lung, kidney, liver, and skin.[52] However, PAI-1 deficiency promotes spontaneous cardiac-selective fibrosis.[52] Our observations of PAI-1 increasing in response to both SPARC overexpression and suppression in TM are analogous to what has been observed in the heart.

These findings, in conjunction with our prior work regarding SPARC overexpression,[13] lead to a set of conclusions regarding the impact of SPARC on various ECM components and regulators within the TM (Table 7). Overexpression of SPARC increases IOP in perfused human anterior segments,[13] transgenic deletion of *SPARC* in mice leads to lower IOPs than in WT mice,[11] and we report in this study that suppressing SPARC lowers IOP in perfused human anterior segments and in WT mice; SPARC regulates IOP. In TM cells, collagen I and IV consistently and directly correlate to SPARC levels (Table 7), but this is not regulated by *COL1* or *COL4* gene expression. TIMP-1 roughly correlates to SPARC levels as well (Table 7). The effect of SPARC on pro-MMP and TIMP levels and on the MMP/TIMP balance determining MMP activity is not yet fully elucidated. To date, the effect of overexpressed SPARC in WT mice has not been published, nor has the zymographic effect on MMP activity, which limits the ability to compare effects across all three model systems.

ECM deposition and turnover are likely regulated by several mechanistic pathways. We have previously shown that SPARC regulates IOP through a coordinated response involving increased levels of certain ECM proteins in conjunction with a selective decrease of enzymatic activity, resulting in qualitative changes in the JCT ECM. The results within this report, along with our previous observation that *SPARC*$^{-/-}$ mice have a lower IOP and enhanced aqueous outflow, strongly implicate a regulatory role for SPARC in IOP. Work is ongoing to determine the upstream and downstream signaling pathways for SPARC in TM as well as the mechanism responsible for these qualitative changes in the JCT ECM. Furthermore, high-intensity staining around

Investigative Ophthalmology & Visual Science

Table 7. Directional Comparison of Relative Transcript and Protein Levels Expressed in Primary Cultured Human TM Cells Following SPARC Overexpression (adSPARC)[13] and SPARC Suppression (shSPARC)

	adSPARC			shSPARC		
	mRNA	**Protein**	**Zymography**	**mRNA**	**Protein**	**Zymography**
Matricellular						
SPARC	Up	Up		Down	Down	
ECM						
Collagen I	NC	Up		NC	Down	
Collagen IV	NC	Up		NC	Down	
Collagen VI	NC	NC		NC	Down	
Fibronectin	NC	NC		NC	NC	
Laminin	NC	NC		NC	NC	
MMPs						
MMP-1		NC	NC	NC	NC	Down
MMP-2		NC	NC	NC	Down	NC
MMP-3		NC		NC	Up	
MMP-9		Down	Down	NC	NC	
TIMPs						
TIMP-1		Up		NC	Down	
TIMP-2		NC		NC	NC	
TIMP-3		NC		NC	NC	
TIMP-4		NC		NC	NC	
Others						
PAI-1		Up		Up	Up	

NC, no change.

Schlemm's canal cells and in collecting channels (data not shown) was observed; it is possible that SPARC may play a role in regulating the resistance beyond the JCT region and is an area of possible future study. Our work demonstrates that SPARC suppression could be pursued as a novel therapeutic target for the treatment of POAG.

Acknowledgments

The authors thank Ajay Ashok and Neena Singh for generously allowing us to utilize their microscope.

Supported by National Eye Institute 5R01EY019654-02 (DJR) and P30EY011373 (VSRC Core Grant) and unrestricted funds from the Research to Prevent Blindness and the Cleveland Eye Bank Foundation.

Disclosure: **W.W. MacDonald**, None; **S.S. Swaminathan**, None; **J.Y. Heo**, None; **A. Castillejos**, None; **J. Hsueh**, None; **B.J. Liu**, None; **D. Jo**, None; **A. Du**, None; **H. Lee**, None; **M.H. Kang**, None; **D.J. Rhee**, None

References

1. Quigley H, Broman AT. The number of people with glaucoma worldwide in 2010 and 2020. *Br J Ophthalmol*. 2006;90(3):262–267.
2. Bahrami H. Causal inference in primary open angle glaucoma: specific discussion on intraocular pressure. *Ophthalmic Epidemiol*. 2006;13(4):283–289.
3. Rudnicka AR, Mt.-Isa S, Owen CG, Cook DG, Ashby D. Variations in primary open-angle glaucoma prevalence by age, gender, and race: a Bayesian meta-analysis. *Invest Ophthalmol Vis Sci*. 2006;47(10):4254–4261.
4. Weinreb RN, Khaw PT. Primary open-angle glaucoma. *Lancet*. 2004;363(9422):1711–1720.
5. Seiler T, Wollensak J. The resistance of the trabecular meshwork to aqueous humor outflow. *Graefes Arch Clin Exp Ophthalmol*. 1985;223(2):88–91.
6. Ethier CR, Kamm RD, Palaszewski BA, Johnson MC, Richardson TM. Calculations of flow resistance in the juxtacanalicular meshwork. *Invest Ophthalmol Vis Sci*. 1986;27(12):1741–1750.
7. Sage EH, Bornstein P. Extracellular proteins that modulate cell-matrix interactions: SPARC, tenascin, and thrombospondin. *J Biol Chem*. 1991;266(23):14831–14834.
8. Blazejewski S, Le Bail B, Boussarie L, et al. Osteonectin (SPARC) expression in human liver and in cultured human liver myofibroblasts. *Am J Pathol*. 1997;151(3):651–657.
9. Delany AM, McMahon DJ, Powell JS, Greenberg DA, Kurland ES. Osteonectin/SPARC polymorphisms in Caucasian men with idiopathic osteoporosis. *Osteoporos Int*. 2008;19(7):969–978.
10. Pichler RH, Hugo C, Shankland SJ, et al. SPARC is expressed in renal interstitial fibrosis and in renal vascular injury. *Kidney Int*. 1996;50(6):1978–1989.
11. Haddadin RI, Oh D-J, Kang MH, et al. SPARC-null mice exhibit lower intraocular pressures. *Invest Ophthalmol Vis Sci*. 2009;50(8):3771–3777.
12. Vittal V, Rose A, Gregory KE, Kelley MJ, Acott TS. Changes in gene expression by trabecular meshwork cells in response to mechanical stretching. *Invest Ophthalmol Vis Sci*. 2005;46(8):2857–2868.
13. Oh DJ, Kang MH, Ooi YH, Choi KR, Sage EH, Rhee DJ. Overexpression of SPARC in human trabecular meshwork increases intraocular pressure and alters extracellular matrix. *Invest Ophthalmol Vis Sci*. 2013;54(5):3309–3319.
14. Swaminathan SS, Oh DJ, Kang MH, et al. Secreted protein acidic and rich in cysteine (SPARC)-null mice exhibit more uniform outflow. *Invest Ophthalmol Vis Sci*. 2013;54(3):2035–2047.
15. Barker TH, Baneyx G, Cardo-Vila M, et al. SPARC regulates extracellular matrix organization through its modulation of integrin-linked kinase activity. *J Biol Chem*. 2005;280(43):36483–36493.
16. Tripathi RC, Li J, Chan WF, Tripathi BJ. Aqueous humor in glaucomatous eyes contains an increased level of TGF-beta 2. *Exp Eye Res*. 1994;59(6):723–727.

17. NikhalaShree S, Karthikkeyan G, George R, et al. Lowered decorin with aberrant extracellular matrix remodeling in aqueous humor and Tenon's tissue from primary glaucoma patients. *Invest Ophthalmol Vis Sci*. 2019;60(14):4661–4669.
18. Gottanka J, Chan D, Eichhorn M, Lutjen-Drecoll E, Ethier CR. Effects of TGF-beta2 in perfused human eyes. *Invest Ophthalmol Vis Sci*. 2004;45(1):153–158.
19. Bollinger KE, Crabb JS, Yuan X, Putliwala T, Clark AF, Crabb JW. Quantitative proteomics: TGFbeta(2) signaling in trabecular meshwork cells. *Invest Ophthalmol Vis Sci*. 2011;52(11):8287–8294.
20. Kang MH, Oh D-J, Kang J, Rhee DJ. Regulation of SPARC by transforming growth factor beta2 in human trabecular meshwork. *Invest Ophthalmol Vis Sci*. 2013;54(4):2523–2532.
21. Swaminathan SS, Oh D-J, Kang MH, Shepard AR, Pang I-H, Rhee DJ. TGF-beta2-mediated ocular hypertension is attenuated in SPARC-null mice. *Invest Ophthalmol Vis Sci*. 2014;55(7):4084–4097.
22. Aihara M, Lindsey JD, Weinreb RN. Aqueous humor dynamics in mice. *Invest Ophthalmol Vis Sci*. 2003;44(12):5168–5173.
23. Aihara M, Lindsey JD, Weinreb RN. Reduction of intraocular pressure in mouse eyes treated with latanoprost. *Invest Ophthalmol Vis Sci*. 2002;43(1):146–150.
24. Rhee DJ, Fariss RN, Brekken R, Sage EH, Russell P. The matricellular protein SPARC is expressed in human trabecular meshwork. *Exp Eye Res*. 2003;77(5):601–607.
25. Lohr C, Kunding AH, Bhatia VK, Stamou D. Constructing size distributions of liposomes from single-object fluorescence measurements. *Methods Enzymol*. 2009;465:143–160.
26. Downey MJ, Jeziorska DM, Ott S, et al. Extracting fluorescent reporter time courses of cell lineages from high-throughput microscopy at low temporal resolution. *PLoS One*. 2011;6(12):e27886.
27. Hernandez-Garcia CM, Chiera JM, Finer JJ. Robotics and dynamic image analysis for studies of gene expression in plant tissues. *J Vis Exp*. 2010;39:1733.
28. Keller KE, Bhattacharya SK, Borras T, et al. Consensus recommendations for trabecular meshwork cell isolation, characterization and culture. *Exp Eye Res*. 2018;171:164–173.
29. Slauson SR, Peters DM, Schwinn MK, Kaufman PL, Gabelt BT, Brandt CR. Viral vector effects on exoenzyme C3 transferase-mediated actin disruption and on outflow facility. *Invest Ophthalmol Vis Sci*. 2015;56(4):2431–2438.
30. Keller KE, Vranka JA, Haddadin RI, et al. The effects of tenascin C knockdown on trabecular meshwork outflow resistance. *Invest Ophthalmol Vis Sci*. 2013;54(8):5612–5623.
31. Ueda J, Wentz-Hunter K, Yue BYJT. Distribution of myocilin and extracellular matrix components in the juxtacanalicular tissue of human eyes. *Invest Ophthalmol Vis Sci*. 2002;43(4):1068–1076.
32. Zhou L, Li Y, Yue BY. Glucocorticoid effects on extracellular matrix proteins and integrins in bovine trabecular meshwork cells in relation to glaucoma. *Int J Mol Med*. 1998;1(2):339–346.
33. Aihara M, Lindsey JD, Weinreb RN. Ocular hypertension in mice with a targeted type I collagen mutation. *Invest Ophthalmol Vis Sci*. 2003;44(4):1581–1585.
34. Choquest H, Thai KK, Yin J, et al. A large multi-ethnic genome-wide association study identifies novel genetic loci for intraocular pressure. *Nat Commun*. 2017;13(8):2108.
35. Wirtz MK, Sykes R, Samples J, et al. Identification of missense extracellular matrix gene variants in a large glaucoma pedigree and investigation of the N700S thrombospondin-1 variant in normal and glaucomatous trabecular meshwork cells. *Curr Eye Res*. 2022;47:79–90.
36. Lutjen-Drecoll E, Rittig M, Rauterberg J, Jander R, Mollenhauer J. Immunomicroscopical study of type VI collagen in the trabecular meshwork of normal and glaucomatous eyes. *Exp Eye Res*. 1989;48(1):139–147.
37. Faralli JA, Filla MS, Peters DM. Role of fibronectin in primary open angle glaucoma. *Cells*. 2019;8(12):1518.
38. Emerson RO, Sage EH, Ghosh JG, Clark JI. Chaperone-like activity revealed in the matricellular protein SPARC. *J Cell Biochem*. 2006;98(4):701–705.
39. Bradley JM, Vranka J, Colvis CM, et al. Effect of matrix metalloproteinases activity on outflow in perfused human organ culture. *Invest Ophthalmol Vis Sci*. 1998;39(13):2649–2658.
40. English JL, Kassiri Z, Koskivirta I, et al. Individual TIMP deficiencies differentially impact pro-MMP-2 activation. *J Biol Chem*. 2006;281(15):10337–10346.
41. Mateo F, Meca-Cortes O, Celia-Terrassa T, et al. SPARC mediates metastatic cooperation between CSC and non-CSC prostate cancer cell subpopulations. *Mol Cancer*. 2014;13:237.
42. Okada Y, Nagase H, Harris EDJ. A metalloproteinase from human rheumatoid synovial fibroblasts that digests connective tissue matrix components: purification and characterization. *J Biol Chem*. 1986;261(30):14245–14255.
43. Oh D-J, Martin JL, Williams AJ, Russell P, Birk DE, Rhee DJ. Effect of latanoprost on the expression of matrix metalloproteinases and their tissue inhibitors in human trabecular meshwork cells. *Invest Ophthalmol Vis Sci*. 2006;47(9):3887–3895.
44. Atorrasagasti C, Peixoto E, Aquino JB, et al. Lack of the matricellular protein SPARC (secreted protein, acidic and rich in cysteine) attenuates liver fibrogenesis in mice. *PLoS One*. 2013;8:e54962.
45. Tripathi BJ, Geanon JD, Tripathi RC. Distribution of tissue plasminogen activator in human and monkey eyes: an immunohistochemical study. *Ophthalmology*. 1987;94(11):1434–1438.
46. Murphy G, Atkinson S, Ward R, Gavrilovic J, Reynolds JJ. The role of plasminogen activators in the regulation of connective tissue metalloproteinases. *Ann NY Acad Sci*. 1992;667:1–12.
47. Hu Y, Barron AO, Gindina S, et al. Investigations on the role of the fibrinolytic pathway on outflow facility regulation. *Invest Ophthalmol Vis Sci*. 2019;60(5):1571–1580.
48. Wong SLI, Sukkar MB. The SPARC protein: an overview of its role in lung cancer and pulmonary fibrosis and its potential role in chronic airways disease. *Br J Pharmacol*. 2017;174(1):3–14.
49. Fleenor DL, Shepard AR, Hellberg PE, Jacobson N, Pang I-H, Clark AF. TGFbeta2-induced changes in human trabecular meshwork: implications for intraocular pressure. *Invest Ophthalmol Vis Sci*. 2006;47(1):226–234.
50. Mao W, Liu Y, Mody A, Montecchi-Palmer M, Wordinger RJ, Clark AF. Characterization of a spontaneously immortalized bovine trabecular meshwork cell line. *Exp Eye Res*. 2012;105:53–59.
51. Konrad L, Scheiber JA, Schwarz L, Schrader AJ, Hofmann R. TGF-beta1 and TGF-beta2 strongly enhance the secretion of plasminogen activator inhibitor-1 and matrix metalloproteinase-9 of the human prostate cancer cell line PC-3. *Regul Pept*. 2009;155(1–3):28–32.
52. Ghosh AK, Vaughan DE. PAI-1 in tissue fibrosis. *J Cell Physiol*. 2012;227(2):493–507.

Investigative Ophthalmology & Visual Science